Packaging for Laser-Based White Lighting: Status and Perspectives

Yupu Ma
School of Energy and Power Engineering,
Huazhong University of Science and Technology,
Wuhan 430074, China

Xiaobing Luo[1]
School of Energy and Power Engineering,
Huazhong University of Science and Technology,
Wuhan 430074, China
e-mail: luoxb@hust.edu.cn

Light-emitting diodes (LEDs) have gained wide adoption in general illumination applications in the last decade. However, the efficiency drop of LEDs with increasing current density limits the luminous flux per wafer area. In contrast, laser diodes (LDs) can achieve higher efficiency at high current density. Likewise, the etendue of LDs is very low due to the small emitting area and divergent angle, facilitating the high-luminance. Hence, LDs may outperform LEDs in future high-luminance solid-state lighting (SSL). However, the rapid development of high-luminance white laser diode (WLD) is still facing some challenges. First, the heat flux of LD chip is extremely high, leading to a higher junction temperature. Second, the laser beam exhibits an elliptical and astigmatic pattern with Gaussian intensity distribution, which may deteriorate the lighting performances. Third, to achieve high-luminance lighting, the laser beam is usually focused onto the phosphor layer, which may easily increase the phosphor temperature to the thermal quenching region. A comprehensive understanding of these problems enables the advancements of packaging designs for WLDs. In this review, we summarized the recent progress in the packaging of WLDs. First, the advantages and applications of LDs were presented. Then, the state-of-the-art methods of generating white light using LDs were reviewed, in terms of packaging structures and performances. Finally, the challenges and corresponding progresses for the packaging of WLDs were overviewed. This review intends to contribute to the development of next-generation high-luminance laser-based white lighting. [DOI: 10.1115/1.4044359]

Keywords: laser diode, packaging, laser-based white lighting, high-luminance, thermal quenching

1 Introduction

Solid-state lighting (SSL) has advanced rapidly in the last decade and has already outperformed the traditional light sources in the lighting market [1]. Light-emitting diode (LED), as the most successful representative of SSL, has gained wide adoption in general lighting and backlight display [2–4]. Despite the great achievements, LED is still suffering from the thermal droop, i.e., a decrease of efficiency in high input current density [5]. This inevitably limits the achievable luminous flux per unit area of the LED chip [6].

As an alternative option of SSL, the laser diode (LD) can provide a solution for the LED efficiency droop. LD can achieve high-efficiency at a much higher current density because the Auger recombination no longer grows after the threshold current [7,8]. Driven by this characteristic, Shuji Nakamura predicted in his Nobel lecture that GaN-based LDs may enable the next-generation SSL [9]. Figure 1(*a*) shows the comparison of the power-conversion efficiency between LED and LD [7]. The efficiency of LED peaks at a relatively low input power density of about 3 W/cm^2, and decreases rapidly with rising input power density. In contrast, the power-conversion efficiency of LD keeps rising with input power density after threshold and exceeds that of the LED at 7 kW/cm^2. This unique feature of LD makes it more competitive in the future high-power SSL.

In addition, LD exhibits other excellent characteristics for SSL. First, LD emits nearly monochromatic light with narrow bandwidth by operating in the stimulated emission [10]. Figure 1(*b*) plots the normalized spectral power distribution of a commercial blue LED [1] and LD [11]. The full width at half maximum (FWHM) of the LED (20 nm) is much higher than that of LD (2.5 nm). Typically, it may raise a question that the narrow linewidth source will have relatively low color rendering quality. To explore the feasibility of LD for white lighting, Neumann et al. have conducted a most extreme configuration by combining four (blue–green–yellow–red) LDs to produce white light [12]. It was demonstrated that the white LD (WLD) can achieve comparable color rendering performance with white LED (WLED). Moreover, the spiky (narrow linewidth) light sources give the theoretically highest luminous efficiency for a given correlated color temperature and color rendering index [13]. Due to the narrow FWHM, LD possesses purer color and wider color gamut than LED and other traditional light sources, e.g., cathode ray tube, liquid crystal display, and LED [14]. This feature makes the LD more competitive in the projection display. For example, Nippon electronic company (NEC) has proposed a laser projector based on red–green–blue (RGB) laser sources shown in Fig. 2(*a*) [15]. Compared with traditional RGB LED projector, the RGB laser projector has higher brightness, higher resolution (native 4 K), and smaller volume. It is a trend that the laser projector is replacing the LED projector in the cinema and also home theater.

Second, the laser beam shows a directional pattern with smaller divergent angle than that of LED with a typical Lambertian pattern. In addition, the LD light emits from a very small aperture (e.g., 1 μm × 10 μm). In this case, the optical energy emitted from LD is much higher than that of LED. Hence, the etendue of the LD can be extremely small and can in principle achieve high-luminance lighting [16]. This paves the way for the use of LD in automotive lighting. BMW (Bayerische, Germany) proposed a headlamp,

[1]Corresponding author.

Contributed by the Electronic and Photonic Packaging Division of ASME for publication in the Journal of Electronic Packaging. Manuscript received November 5, 2018; final manuscript received July 19, 2019; published online September 19, 2019. Editor: Y. C. Lee.

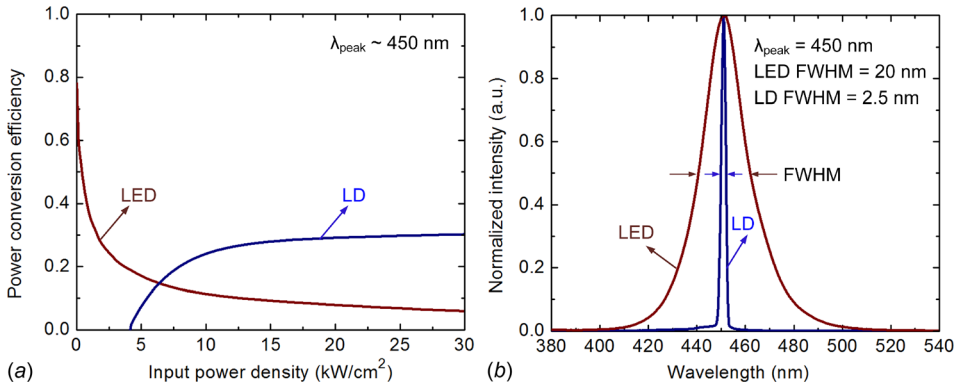

Fig. 1 Comparison between blue LED and blue LD (with a peak wavelength of 450 nm): (*a*) the power-conversion efficiency versus input power density [7] and (*b*) the normalized spectral intensity distribution [1,11]

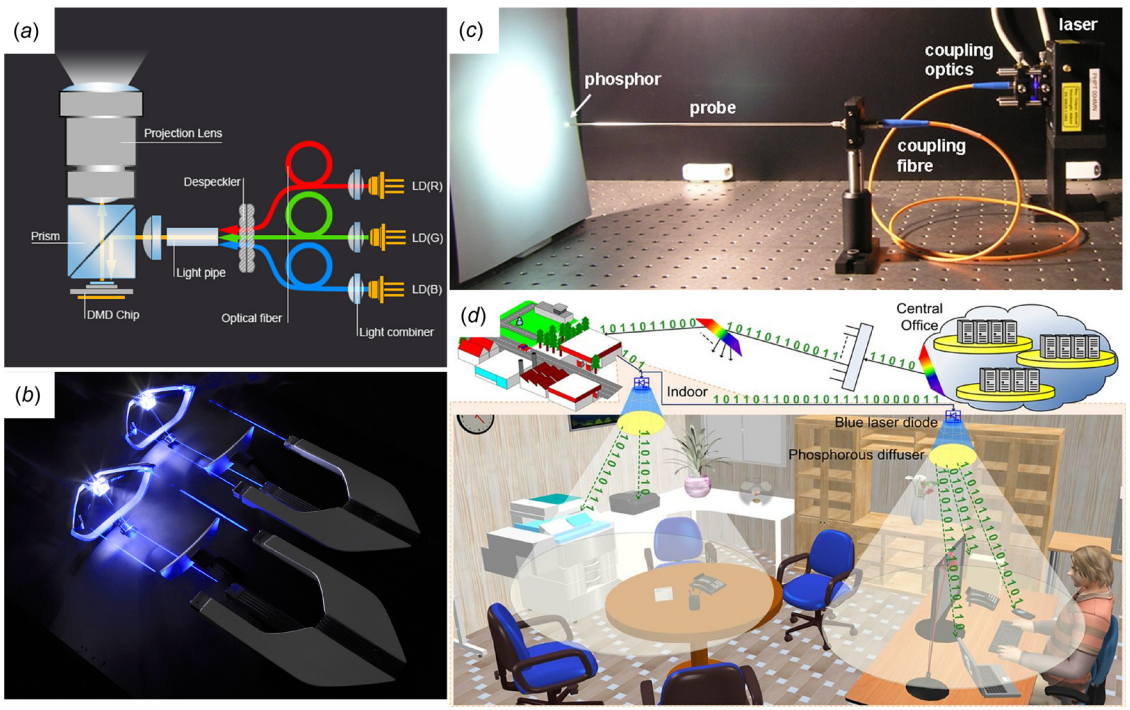

Fig. 2 The applications of LDs in (*a*) NEC laser projector [15], (*b*) BMW laser headlight [17], (*c*) medical endoscopic illumination source [21], and (*d*) visible light communication [22]

shown in Fig. 2(*b*), by using a blue LD excited the remote phosphor in the i8 concept car in 2011 [17]. It was reported that the laser-based headlamp was much brighter and efficient than LED-based counterparts [18]. And the visual range of laser beam is 600 m, compared with 300 m for LED high-beam [19]. Also, Audi demonstrated a laser-based tail light in the consumer electronics show in 2013 [20]. In the following, Mercedes-Benz displayed a concept sports utility vehicle with a laser projection-based front lighting system in 2013 [21]. Therefore, the LD has started to gain attention and will distinguish itself in the future automotive industry.

Third, the laser beam is easier to be controlled, either collimated/focused or expanded, which may facilitate the optics design [16]. Usually, it is easier and more efficient to couple the laser beam into an optical fiber than LED. Nadeau et al. have proposed a laser-based endoscopic illumination source for medical application [21]. As shown in Fig. 2(*c*), the endoscopic light source is designed by coupling the laser beam with a fiber to excite a remote phosphor plate coated onto the other end of the fiber [21]. This approach is reported to offer a more compact design and sharper image formation than the standard endoscope illumination sources. In addition, the modulation rate of LD is higher than that of LED, making LD suitable for remote communication. Recently, the visible light communication based on LD has been a research hotspot [22–24]. As shown in Fig. 2(*d*), both lighting and optical communication can be simultaneously achieved through the light-fidelity (LiFi) system [22]. Progresses have been made to pursue high communicate rate and high bandwidth.

It should be noted that the laser beam has high coherence due to the nature of stimulated radiation, which may result in some visible effects. The most common effect is the laser speckle, which is created when the coherent light reflects from a sufficiently rough surface. Fortunately, Aquino et al. have revealed that speckle is not of concern in illumination for LD-based phosphor-converted white light sources [25].

From the above introductions, LD is a very promising candidate in the future high-power and high-luminance SSL. However, to

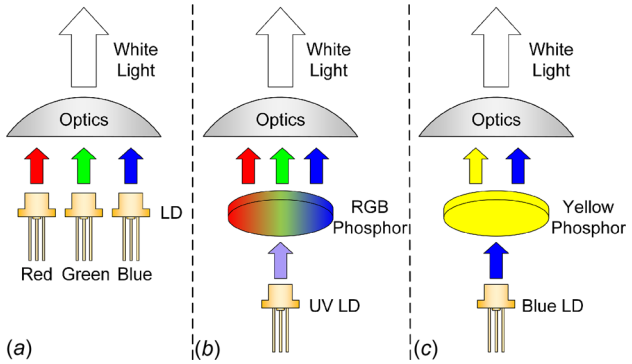

Fig. 3 The schematic of three types of methods to achieve WLDs: (*a*) RGB LDs, (*b*) UV LD + RGB phosphors, and (*c*) blue LD + yellow phosphor

quickly penetrate the applications, many packaging issues of the WLD need to be solved. The heat flux in the LD chip junction can be very high and efficient thermal management of LD is needed to maintain a relatively lower junction temperature [26]. In addition, the elliptical and astigmatic laser beam is not favorable in far field lighting and laser beam shaping process is needed to obtain the desired high-quality lighting performance. Moreover, the optical energy density in the phosphor layer exposed to LD can be very high, in which case the phosphor thermal quenching can occur easily [27]. A comprehensive understanding of these problems enables the advancements of the packaging processes involving thermal management, optics design, material science, processing, mechanical design, and optical–thermal interactions. Some books on the packaging of high power semiconductor lasers have been published [28]. In addition, Wierer et al. reviewed the comparisons of the physics and efficiency between LEDs and LDs [7]. Chellappan et al. overviewed the laser-based application for displays [14]. To the of our best knowledge, there is still no published literatures dedicated to the packaging of high power WLDs. Therefore, in this review, the status and perspectives of the packaging aspects of laser-based white lighting were presented. Herein, the state-of-the-art packaging technologies of WLDs was introduced, followed by the challenges and corresponding progresses for WLDs.

2 Packaging of White Laser Diodes

Similar with WLEDs, there are three ways of achieving WLDs. As shown in Fig. 3(*a*), the first concept is to mix multiple color (RGB or red-yellow-green-blue ((RYGB)) LDs and then generate white light [12,29–32]. This configuration can obtain comparable color quality with WLED [12]. However, the multiple LDs not only increase the cost considering the expensive price of the commercial LD chip, but also deteriorate the reliability of the optical system considering the varying working performances of the multiple LDs. Alternatively, using a LD to excite the phosphor has been presented to generate white light, which includes two categories. As shown in Fig. 3(*b*), one type is using a UV LD to excite RGB phosphors [8,33–39], and the mixture of converted RGB colors results in white light. The other type is using a blue LD to excite the yellow phosphor [6,35,40–57], as shown in Fig. 3(*c*), and the converted yellow light mixes with the transmitted blue light, thus generating white light. Table 1 summarizes the recent progresses in developing WLDs using a UV LD to excite RGB phosphor and a blue LD to excite yellow cerium-doped yttrium aluminum garnet (YAG: Ce) phosphor. In general, the former type has higher color rendering index but relatively lower luminous efficiency due to multiple absorptions. The latter type is the most applied way with the advantages of high luminous efficiency, low cost, and compact size.

Due to the extremely high heat flux exceeding 10^8 W/m^2 of LD chip, the remote phosphor configuration is always applied to avoid the phosphor overheating by the chip. The laser-excited remote phosphor (LERP) consists of two common types including the transmissive type and the reflective type [58,59]. As shown in Fig. 4, for the transmissive LERP, the phosphor layer is coated onto a transparent substrate [27] and the light will penetrate through the layer. In some cases, the transparent substrate is not applied, and the side of the phosphor layer is fixed [43]. For the reflective LERP, the phosphor layer is coated onto a mirror layer or a reflective substrate [27] with high specular reflectivity and the light will be reflected in the phosphor–substrate interface. It has been reported in our previous literature that reflective type exhibited higher luminous efficiency because there was backward light energy loss in the transmissive type [58]. Moreover, the reflective type possesses higher thermal stability with lower phosphor temperature and enables flexible optical-thermal design [58]. Therefore, the reflective pc-LD can be more competitive than transmissive type in the future high-luminance lighting industry.

Table 1 Recent progresses in developing WLDs using a UV LD to excite RGB phosphor and a blue LD to excite YAG: Ce phosphor

λ_{ex} (nm)	Phosphor type	Correlated color temperature (K)	Ra	Φ_v (lm)	η_v (lm/W)	Year	Ref.
405	RGB	5200	70	5.7	13	2008	[33]
402		3600	91	47	16	2013	[35]
415		2860	97	/	/	2015	[8]
404		5586	/	/	/	2016	[37]
410		4050	79	/	/	2017	[39]
445	YAG: Ce	5200	60	113	44	2010	[41]
442		4400	57	252	76	2013	[35]
442		7300	62	1100	86.7	2015	[6]
445		3932	/	/	64.7	2015	[42]
450		7045	/	250	45	2015	[43]
450		7373	61.5	/	/	2015	[44]
450		6314	/	1093	48.9	2016	[46]
450		6403	68	/	40	2016	[47]
445		5649	/	/	110	2017	[50]
455		6990	56	850	70	2017	[52]
450		6504	74	1839	/	2018	[53]
450		5666	60.8	/	23.8	2018	[54]
450		6230	62.5	/	26.5	2019	[55]
450		6593	/	369	/	2019	[56]
445		3646	57	651	/	2019	[57]

λ_{ex} denotes the peak excitation wavelength of LD, Φ_v, and η_v are luminous flux and luminous efficiency, respectively.

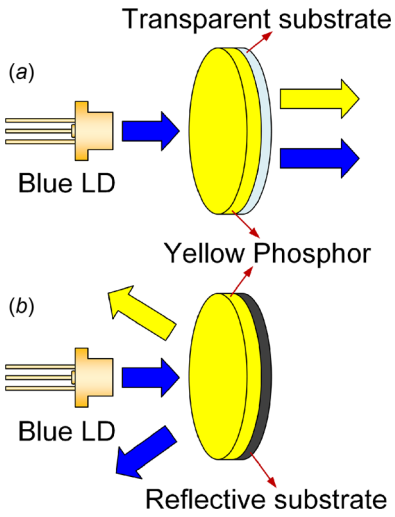

Fig. 4 The schematic of the (*a*) transmissive and (*b*) reflective laser-excited remote phosphor

It should be noted that there is also another LERP type by coupling the laser beam into a fiber to excite the remote phosphor layer [21].

In this part, the LERP is selected as an example to illustrate the packaging structure and process for WLDs. Figure 5 shows the typical structure of a transmissive LERP, which consists of a blue LD module, laser beam shaping optics, a phosphor module, secondary optics, and encapsulation. The remote phosphor configuration allows the separate optical and thermal designs of the LD module and phosphor module. Hence, the packaging process of WLDs is quite simple and is as follows. First, as shown in Fig. 5(*b*), the LD is fabricated through die bonding, wire bonding, and assembling with an internal heat sink and a protective can. The light is edge-emitted from the active region, and the generated heat is then conducted to the internal heat sink. The details of packaging processes for LD chip can be found in the published book [28]. Due to the high heat flux, the LD needs to be assembled with a heat dissipation element, such as external heat sink, thermo-electric cooler, or liquid cooling microchannel. Second, the laser beam shaping optics system (usually collimated or focused lens) is designed based on the requirements to enhance the laser beam quality. Third, the phosphor plate, usually in the shape of thin film, is fabricated using spin-coating method [60], screen printing method, or other methods adopted in WLEDs [1]. As shown in Fig. 5(*c*), the fabricated phosphor film is then coated onto a transparent substrate or fixed in a phosphor holder by the edge. Fourthly, the secondary optics system (e.g., reflector or free-form lens) is designed to extract the white light and obtain the desired lighting performance. Finally, these components are mounted onto the encapsulation according to the design requirements, especially the relative position of the beam shaping lens and secondary optics. The encapsulation provides support and protection of the LD chip, optics, and phosphor. Figure 6 shows the typical structure of a reflective LERP. Compared with the transmissive LERP, the reflective LERP has same components but different phosphor module and optical path. As shown in Fig. 6(*c*), the fabricated phosphor film is usually coated onto a reflective substrate. The reflective substrate serves as the support and the heat dissipation path for the phosphor film. It should be noted that additional heat dissipation elements can be applied to further lower the phosphor temperature and thus maintain high performances. In addition, the collimated laser beam from the beam shaping optics usually excites the phosphor film at a certain angle (e.g., 10 deg∼70 deg) in the convenience of light extraction. The secondary optics design also needs to be altered according to the requirements. The packaging process of the reflective LERP is very similar with that of the transmissive LERP. From the above packaging process, we can see that the good optical performances depend on the good design of thermal management, optics, color mixing, material, and especially taking into account of the unique characteristics of LD mentioned above.

3 Challenges in White Laser Diodes

From the packaging processes presented in Sec. 2, there are three key problems to be addressed in WLDs' packaging and applications.

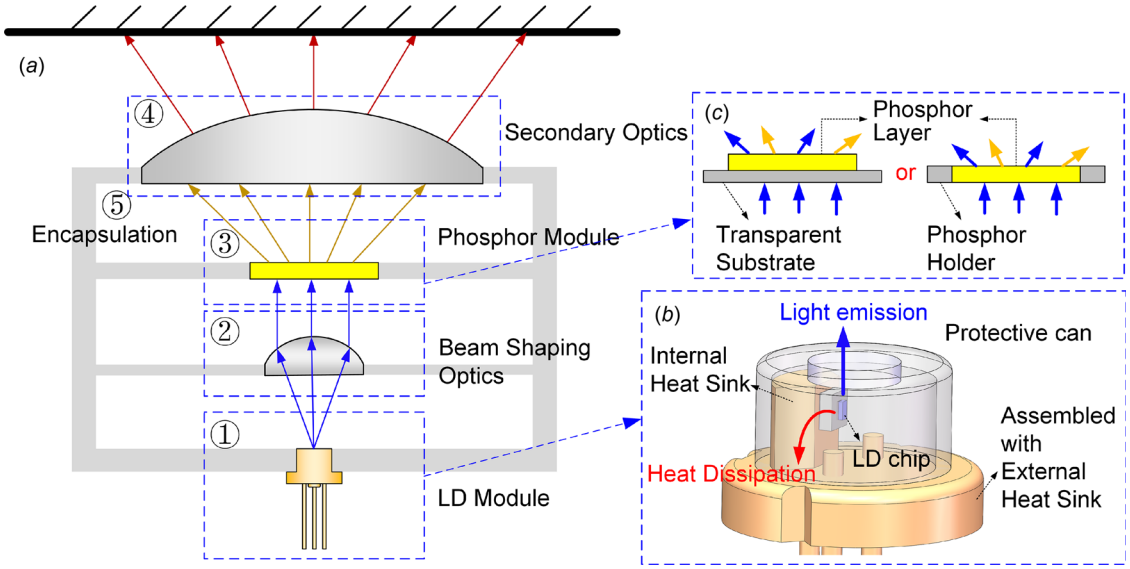

Fig. 5 (*a*) The typical packaging structure of transmissive LERP consisting of: (1) a blue LD module, (2) laser beam shaping optics, (3) a phosphor module, (4) secondary optics, and (5) encapsulation. (*b*) The enlarged figure of the LD module consisting of a blue LD and an external heat sink (not shown) assembled around the protective can. (*c*) The enlarged figure of the transmissive phosphor module consisting of the phosphor layer coated onto a transparent substrate or fixed in a phosphor holder by the edge.

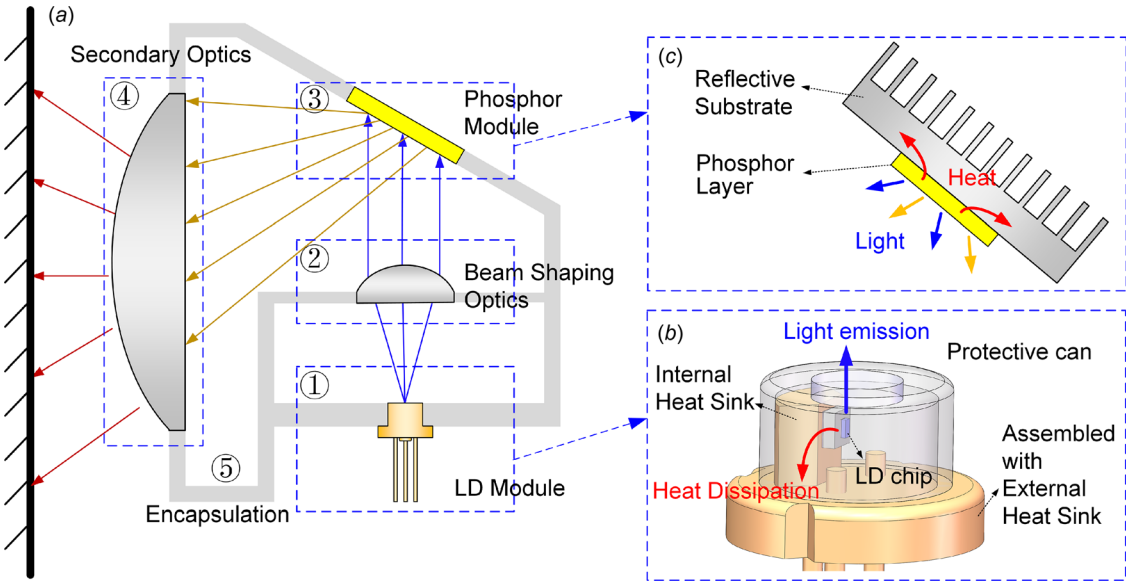

Fig. 6 (*a*) The typical packaging structure of reflective LERP consisting of: (1) a blue LD module, (2) laser beam shaping optics, (3) a phosphor module, (4) secondary optics, and (5) encapsulation. (*b*) The enlarged figure of the LD module consisting of a blue LD and an external heat sink (not shown) assembled around the protective can. (*c*) The enlarged figure of the reflective phosphor module consisting of the phosphor layer coated onto a reflective substrate.

3.1 High Heat Flux of Laser Diode. According to the Fourier heat conduction law, the junction temperature of LD T_j can be expressed as

$$T_j = T_a + R_{th} \cdot Q_{LD} \tag{1}$$

where T_a is the ambient temperature, and R_{th} is the total thermal resistance from the chip junction to the ambient, which is the sum of the thermal resistance for each bulk layer, thermal interface resistance, and thermal spreading resistance [61]. Q_{LD} denotes the heat generation power in the chip and can be simply calculated as the subtraction of the total input electrical power P_{in} to the output optical power P_{out} [3,62]

$$Q_{LD} = P_{in} - P_{out} = I_0 V_0 \cdot (1 - \eta_{wp}) \tag{2}$$

where P_{in} is the product of the input current I_0 and input voltage V_0, and η_{wp} is the power-conversion efficiency.

However, the efficiency of the state-of-the-art blue LD is relatively low, just as the case with LED in ten years ago. Even driven at high power density (15 kW/cm^2), as shown in Fig. 1(*a*), η_{wp} is about 0.3 with a corresponding high heat flux of LD chip in the order of 10^8 W/m^2. Due to the demand of high output power, the input power needs to be increased and a considerable amount of heat can be generated, resulting in very high temperature rise in the chip junction. As with LEDs, higher junction temperature of LDs reduces the carrier confinement and increases the nonradiative recombination rate [28]. Both effects lead to a higher threshold current and a lower conversion efficiency, thus limiting the maximum output power. Figure 7 shows the output optical power of a single diode laser versus current at different temperatures [63]. We can see that the output power decreases constantly with rising temperature. Moreover, high junction temperature will lead to red-shift, i.e., the output wavelength shift toward longer wavelength region [64]. Also, the reliability and lifetime will be reduced due to the high junction temperature.

Therefore, lower junction temperature (<70 °C) is very essential to maintain high output power and high performance of LD. The extremely high heat flux in the LD chip makes the thermal management challenging.

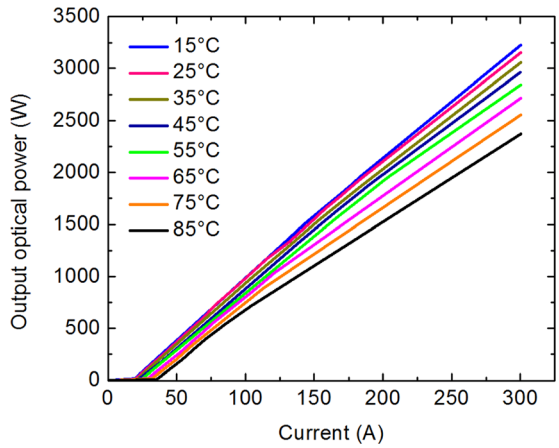

Fig. 7 The output optical power of a single LD versus current at different temperatures [63]

3.2 Poor Beam Quality. Figure 8 shows the laser beam pattern from an edge-emitting semiconductor LD [65]. It is obvious that the laser beam has an elliptical shape, i.e., the divergent angles in the perpendicular and parallel directions are different. Typically, the FWHM divergent angles are ~30 deg along the perpendicular direction ($\theta_\perp$) and ~8 deg along the parallel direction ($\theta_\parallel$), respectively [28]. Moreover, the laser beam is astigmatism, which means that the virtual point sources appear in two different locations in the perpendicular and parallel directions [66]. The elliptical and astigmatism laser beam is due to the fact that the aperture size in the parallel direction is an order of magnitude larger than that in the perpendicular direction in the active region. It should be noted that after a long-range propagation, the difference between these two directions can be further increased, resulting in a highly elliptical beam shape at the far field. If a phosphor sample is illuminated by this elliptical laser beam, the intensity and spot diameter along these two orthogonal directions of the output white light may differ from each other very much, which is not favorable for the follow-up secondary optics design and good

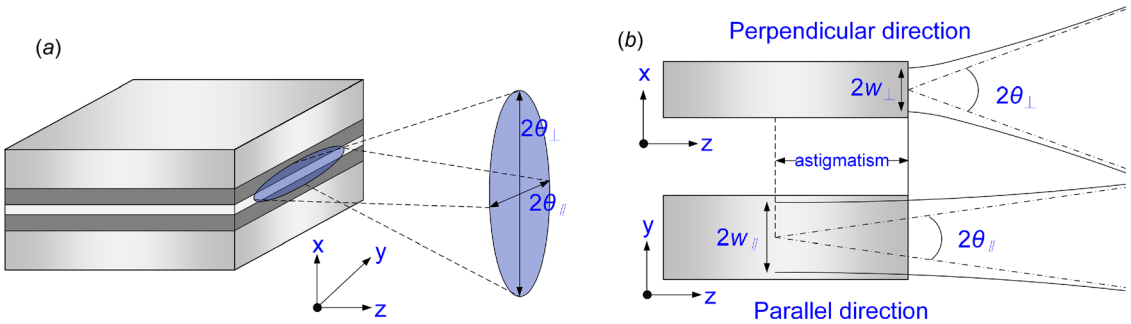

Fig. 8 (*a*) Free-space radiation pattern of an edge-emitting LD with an elliptical beam profile, and (*b*) the laser beam propagating along perpendicular and parallel directions. The astigmatism is illustrated by the difference along propagation (*z*-) axis between two virtual point sources [65].

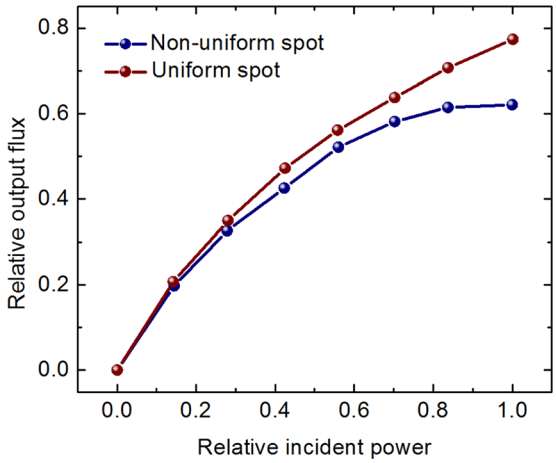

Fig. 9 Relative emitted flux from phosphor versus input power excited by nonuniform and uniform laser spot [34]

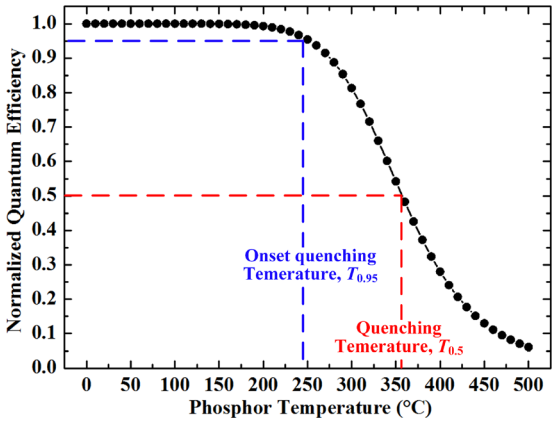

Fig. 10 The typical temperature-dependent quantum efficiency of the commercial YAG: Ce phosphor [11,70]. The onset quenching temperature ($T_{0.95}$) and quenching temperature ($T_{0.5}$) are defined as the temperature corresponding to 95% and 50% of the peak QE, respectively.

lighting quality. In addition, most lasers have Gaussian irradiance distribution [67]. When excited by this type of laser beam, the central region of the phosphor is illuminated by the most of the energy, while the outer region of the phosphor is illuminated by only a small portion of the energy. In this case, the energy utilization efficiency can be relatively low. Figure 9 shows the comparison between the emitted flux from the phosphor excited by the nonuniform and uniform laser spot versus different input power [34]. We can see that the uniform spot can achieve higher flux than the nonuniform spot.

As a whole, the poor beam quality is a bottleneck limiting the further applications of WLDs. Circular and uniform laser beam without astigmatism is pursued for efficiently pumping the phosphor and thus obtaining high-quality white light.

3.3 Phosphor Thermal Quenching. As mentioned above, LD is a competitive candidate in high-power and high-luminance SSL. Usually, to obtain high brightness, the laser beam is collimated or focused onto the phosphor layer with a very small spot, resulting in a very high excitation intensity [68]. When light penetrates through the phosphor layer, part of the optical energy may be converted into heat due to the quantum efficiency loss, Stokes shift loss, and absorption loss by the packaging structures [1]. This is also known as phosphor heating [68], which may further result in high phosphor temperature due to the relatively low thermal conductivity of the organic binders [69]. The basic problem with pumping a fluorescent material at high excitation flux is that the quantum efficiency begins to decrease rapidly above a certain temperature. Figure 10 plots the typical temperature-dependent quantum efficiency (QE) of the commercial YAG:Ce phosphor [11,70]. As the temperature increases, the QE remains stable at first and then starts to decrease quickly above the onset quenching temperature $T_{0.95}$ corresponding to 95% of the peak QE. The decrease of quantum efficiency leads to a rise of heat generation in the phosphor layer and also increment of the phosphor temperature, and conversely results in a further decline of QE. This thermal runaway effect finally leads to a higher phosphor temperature far exceeding quenching temperature $T_{0.5}$ corresponding to 50% of the peak QE. This phenomenon is known as the phosphor thermal quenching [70], which will decrease the efficiency, deteriorate the reliability, and shorten the lifetime of WLDs [27].

To investigate the thermal quenching effect, we proposed an optical–thermal coupling model to predict the phosphor temperature of the reflective LERP [11]. Figure 11 shows the schematic of the optical–thermal model comprising the phosphor scattering model and the thermal resistance model. The phosphor heat generation Q_{ph} is calculated using the phosphor scattering model based on the modified Kubelka–Munk theory [71–74]. By inputting the phosphor heat generation into the thermal resistance model, the phosphor temperature is derived as

$$T_{\text{ph}} = T_a + R_{\text{total}} \cdot Q_{\text{ph}} \tag{3}$$

where R_{total} is the total thermal resistance from the phosphor to the ambient. Moreover, the temperature-dependent quantum efficiency is considered to iteratively calculate Q_{ph} and T_{ph}. Using this model, we calculated the phosphor temperature and output optical power with varying input optical power from LD. As shown in Fig. 12, the output power and phosphor temperature rise

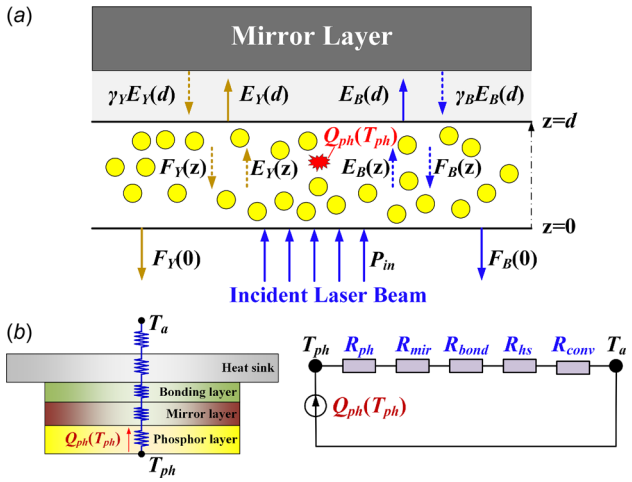

Fig. 11 The optical–thermal coupling model of the reflective LERP considering the phosphor thermal quenching effect [11]. The coupling model consists of (*a*) the phosphor scattering model based on the modified Kubelka–Munk theory and (*b*) the thermal resistance model.

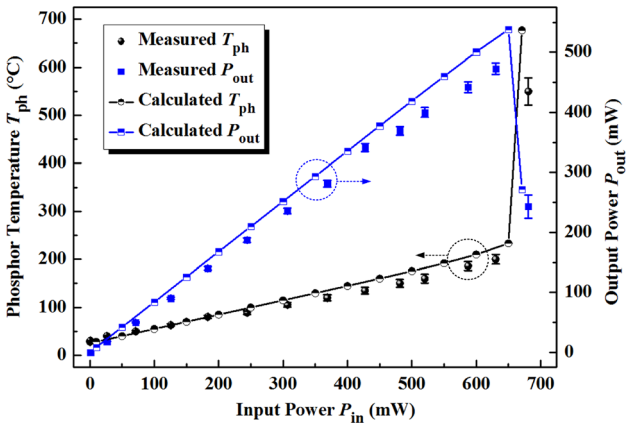

Fig. 12 The calculated and measured phosphor temperature and output optical power versus input power [11]

first with rising input power. However, sudden changes happen after the input power exceeds a critical value. With input power varying from 650 mW to 680 mW, the output power shows a rapid drop from 473 mW to 243 mW, corresponding to a sudden rise of phosphor temperature from 198.0 °C to 549.0 °C. This high phosphor temperature may finally lead to silicone carbonization [11]. As for the transmissive LERP, the phosphor thermal quenching may be more severe compared with the reflective LERP due to the poor heat dissipation ability without highly conductive substrate [58]. The sudden reduce of output optical power and sudden increase of phosphor temperature were also observed for the transmissive LERP, corresponding to a final silicone carbonization phenomenon [58,74].

Therefore, the phosphor temperature may easily reach the thermal quenching region under high excitation flux of LD, and the overall optical–thermal performances may be deteriorated. This challenging issue needs to be addressed in the packaging design process.

4 Progresses in White Laser Diodes

4.1 Laser Diode Thermal Management. Before application of LD in WLDs, the thermal management of LD needs to be resolved to achieve lower junction temperature, and thus a stable

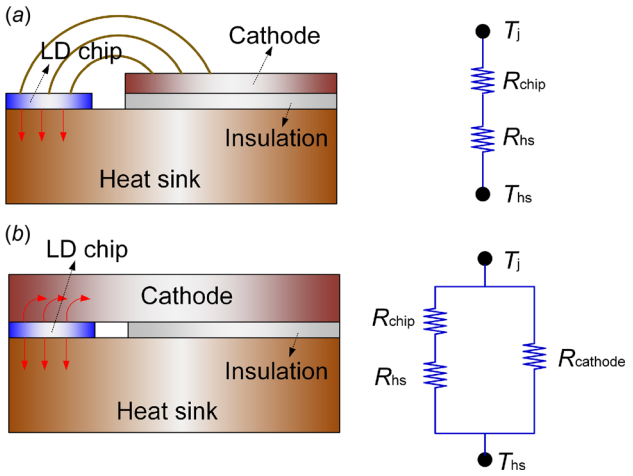

Fig. 13 Left: (*a*) the traditional and (*b*) double-sided cooling packaging structures [75]. Right: The corresponding simplified thermal resistance network.

output and high performance. According to Eqs. (1) and (2), the lower junction temperature can be achieved either by reducing the total thermal resistance R_{th} or increasing the power-conversion efficiency. In this section, we mainly discussed the packaging designs to reduce R_{th}. Three methods were presented to reduce the thermal resistance from chip to substrate, the substrate thermal resistance, and the thermal resistance from the substrate to the ambient, respectively.

4.1.1 Double-Sided Cooling of LD Chip. The LD chip is usually bonded onto an internal heat sink or substrate so that the generated heat can be dissipated to the ambient efficiently. In this traditional case, the chip is cooled only on the bottom side. In order to improve the heat dissipation ability, a double-sided cooling method was proposed [75]. As shown in Fig. 13, for the double-sided cooling scheme, the generated heat in the chip can be conducted through both the cathode and anode. In this design, the traditional thermal resistance path is in parallel connection with another thermal resistance path. Thus, the thermal resistance from the chip to the substrate can be reduced. It has been reported that the total heat dissipation efficiency can be enhanced by 20% [75].

4.1.2 High Thermal-Conductivity Materials. To reduce the thermal resistance of substrate, selecting substrate material with high thermal conductivity has been the most efficient way. Copper, with a thermal conductivity of ~400 W m^{-1} K^{-1}, has been widely used as substrate material in semiconductor electronic packaging. In order to further improve the heat dissipation performance, other substrate materials with higher thermal conductivity have been studied. The diamond has been a very promising heat-conductive material due to its extremely high thermal conductivity of 2000 W m^{-1} K^{-1}. Limited by the cost of the diamond, the copper and diamond compound has been produced in recent years. The thermal conductivity of copper and diamond compound can reach 700 W m^{-1} K^{-1} [76], which enhances the heat dissipating efficiency compared to that of the traditional copper substrate.

4.1.3 Liquid Cooling. The heat dissipation from the substrate to the ambient has always been the major part in thermal management design. Several cooling methods have been applied, including the large-area heat sink by natural air cooling or the integrated fan by forced air cooling [77]. However, due to the limited heat dissipation ability, these methods cannot meet the cooling requirements of LD. Thermo-electric cooling has been usually applied in most of the commercial high-power LD cooling system [78].

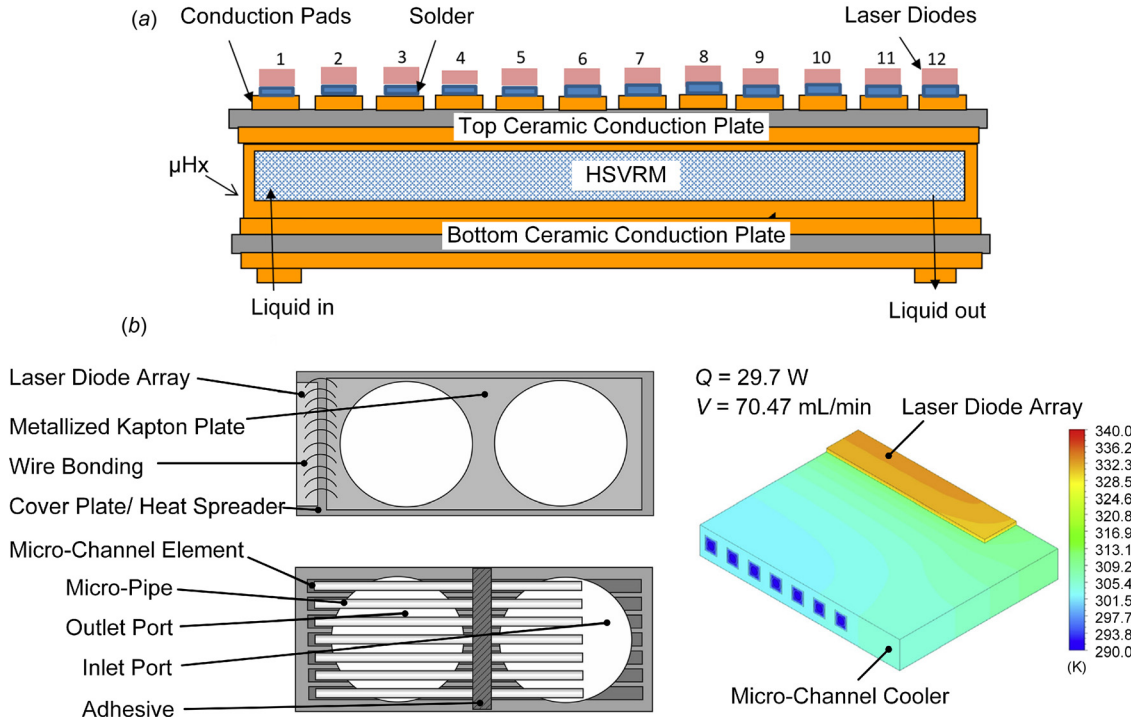

Fig. 14 (*a*) Schematic diagram of the microheat exchanger (μHx) for cooling a high power laser diode array consisting of 12 LDs [80]. (*b*) Schematic diagram of the upper and bottom part of the microchannel cooler with microheat-pipes for cooling high power LD array, and the temperature distribution of the microchannel cooler and laser diodes [81].

However, it requires considerable energy to obtain lower temperature and the cooling capacity of thermo-electric cooling may not meet the requirement for high-power LDs [79]. Therefore, many thermal management methods of LD using liquid cooling have been proposed, recently [80–82]. Datta and Choi presented a liquid cooled microheat exchanger for cooling a high power laser diode array [80]. As shown in Fig. 14(*a*), the heat generated in the LD array was extracted by flowing a cooling liquid through the microheat exchanger. And this cooling system provided low junction temperature, uniform liquid flow, and heat transfer rate over a large surface. Also, Kozłowska et al. proposed a microchannel cooler with microheat-pipes for cooling high power LD array [81]. As shown in Fig. 14(*b*), the micropipes, linking the inlet port and outlet port, served as a highly conductive path for the generated heat in the LD array, thus making the temperature distribution more uniform. It is found that the maximum junction temperature is 67 °C when the heating power is 29.7 W, and the flow rate is 70.47 mL/min, with a corresponding heat remove density of 2.97×10^6 W/m^2 [81]. Therefore, the liquid cooling scheme provides efficient heat dissipation ability and the junction temperature of the high power LD can be maintained at a relatively low range.

4.2 Laser Beam Shaping. To enhance the laser beam quality, the beam shaping process is needed to obtain a circular laser beam with uniform intensity distribution and without astigmatism. The laser beam may be either collimated, focused, or expanded according to the requirement. Researchers have proposed many laser beam shaping methods in the past years, including refractive [83] or reflective systems [84], diffractive elements [85], holograms [86], and microlens system [87–89]. Among them, the refractive laser beam shapers have been widely applied with the advantage of simple structure, high optical efficiency, and less wavelength-dependence [90]. In general, there are two types of refractive laser beam shapers including two plano-aspheric lenses [65,91,92] and a single aspherical lens [92–94]. The optical design approach is based on geometrical ray optics approximation.

Figures 15(*a*) and 15(*b*) show a typical beam shaping system consisting of two aspherical lenses [65]. The front surface of the first lens is a rotationally symmetric surface so that the beam can be collimated in both transverse directions. Then, the elliptical beam is transformed into a circular shape through refraction at the back surface of the first lens and the front surface of the second lens. The beam is re-collimated at the front surface of the second lens and finally travels through the back planar surface of the second lens in both transverse directions. Figures 15(*c*) and 15(*d*) shows the calculated irradiance distribution at different propagation planes. It can be seen that the laser beam has a Gaussian irradiance distribution at the laser output plane. Through beam shaping, the laser beam possesses a uniform irradiance distribution at the output reference plane. Moreover, the elliptical beam is transformed to a circular beam, demonstrating the feasibility of two-lens system in laser beam shaping.

Alternatively, there is another beam shaping system consisting of only one aspherical lens, as shown in Figs. 16(*a*) and 16(*b*) [92]. The front surface has two different refractive powers and surface functions in both transverse directions. Along the perpendicular direction, the beam is collimated at the front surface. Along the parallel direction, the beam propagates through the front surface without refraction. The back surface is flat in the perpendicular direction allowing the beam to propagate directly, while the surface in parallel direction collimates the beam. Figures 16(*c*) and 16(*d*) shows the beam spots at different propagation planes by applying the single-lens system. It can be seen that the input beam at the laser source exit plane is elliptical, whereas the output beam at far field (1 km distance) is transformed to a circular shape.

It should be mentioned that the two-lens system is more practical when there is a large difference between the transverse divergence angles and large output beam spot. On the contrary, when the difference is small, the single-lens system is favorable with

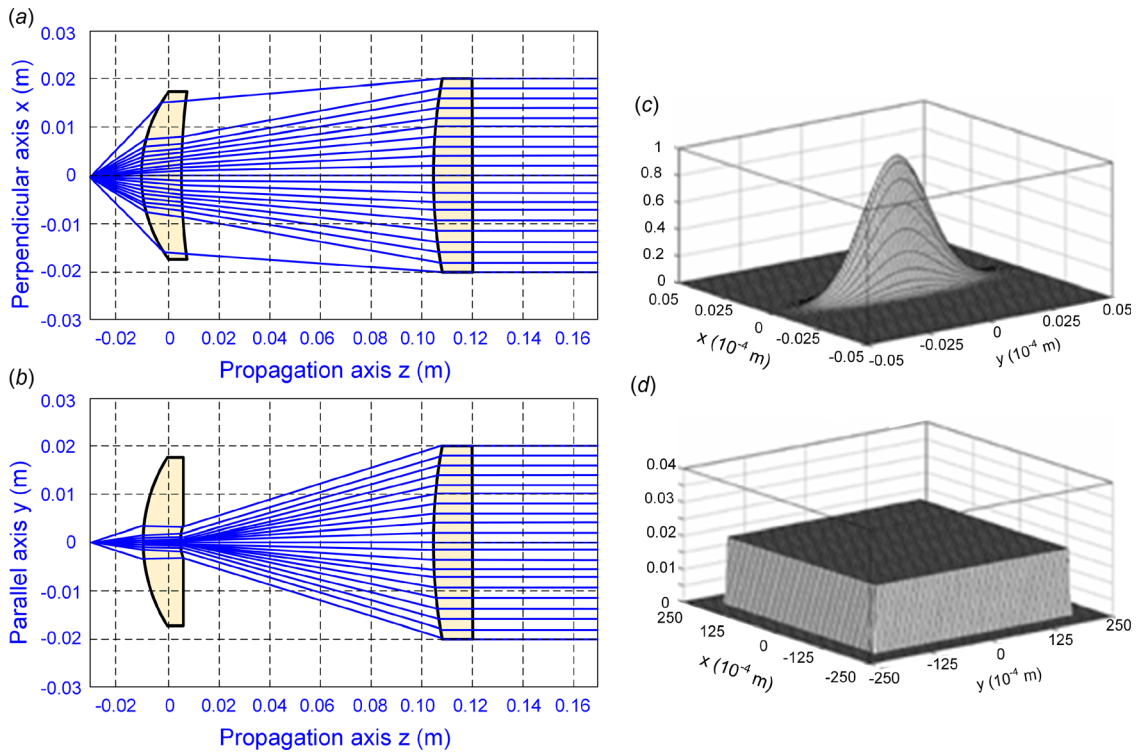

Fig. 15 Ray-tracing results for the two-lens system in the (*a*) *x–z* plane, and (*b*) *y–z* plane. The irradiance distribution at (*c*) the laser output plane, and (*d*) the output reference plane [65].

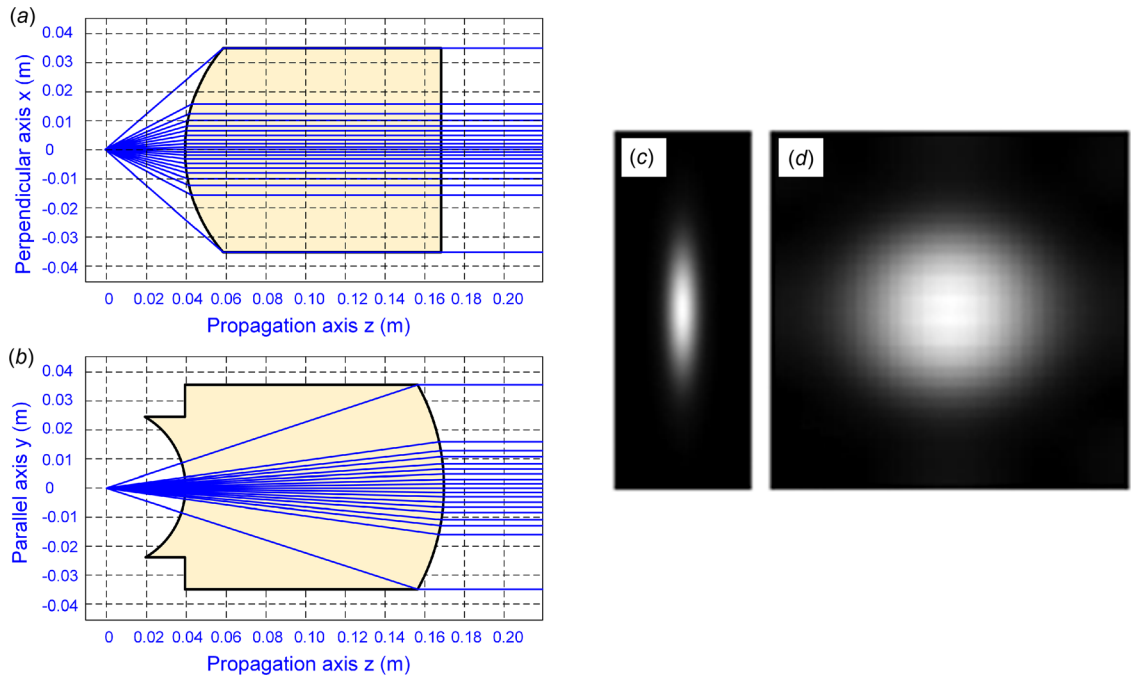

Fig. 16 Ray-tracing results for the single-lens system in the (*a*) *x–z* plane, and (*b*) *y–z* plane. The simulated beam spot using the single-lens system at (*c*) the laser output plane (window size: 4 μm × 10 μm), and (*d*) the output reference plane at 1 km distance (window size: 8 cm × 8 cm) [92].

the advantage of smaller volume. Also, for some applications, the laser beam is required to be coupled into the fiber for remote phosphor excitation and communication. Researchers have developed some fiber coupling methods, including the direct fiber coupling [95], free-space coupling [96], and graded-index lens [97]. The principle of the fiber coupling scheme is to collimate the laser beam along the perpendicular direction and then couple the laser beam into a fiber with a diameter equal to the emitting size from the LD along the perpendicular direction. In addition, through the above beam shaping process, the fiber coupling can be also achieved easily.

4.3 Phosphor Thermal Quenching Relieving. As presented in Sec. 3.3, the phosphor thermal quenching severely reduces the

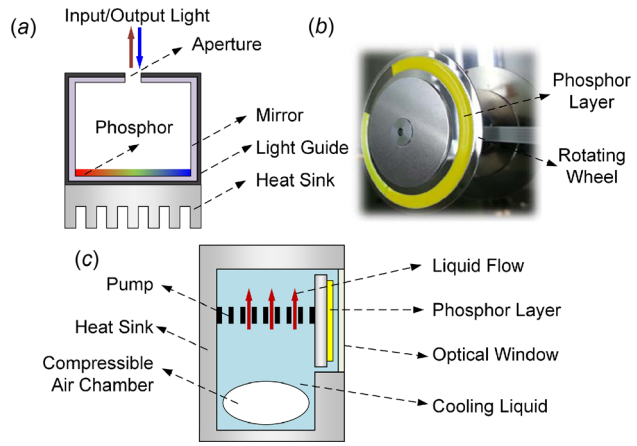

Fig. 17 (*a*) The cross-sectional view of a cylindrical optical cavity consisting of a light guide coated with RGB phosphor layer and heat sink [36], (*b*) photographs of a phosphor layer coated onto a rotating wheel [42], and (*c*) schematic diagram of a sealed liquid cooling system for phosphor layer [49]

output power and even causes failure of the phosphor material. In general, reducing the operating phosphor temperature and enhancing the thermal stability of the phosphor are two ways to relieve the phosphor thermal quenching. Herein, the lower phosphor temperature can be achieved by phosphor thermal management. And the enhancement of the thermal stability can be achieved by selecting the thermally stable phosphor material.

4.3.1 Phosphor Thermal Management. As mentioned previously, the remote phosphor configuration is the commonly used packaging form in LERP, which allows the separate design of LD and phosphor. Hence, it is a natural idea to come up with the concept of thermal management for the phosphor aiming at reducing the phosphor temperature. The most common thermal management design is simply attaching the phosphor layer to a substrate with high thermal conductivity [11,27]. By applying this scheme, the whole system is usually in reflective type, i.e., there is specular or diffuse reflection at the phosphor–substrate interface. Driven by this idea, as shown in Fig. 17(*a*), Abu-Ageel et al. proposed a WLD by using 405 nm/445 nm mixed lasers to excite the RGB phosphor deposited onto a highly reflective mirror at the bottom side of a light guide [36]. And the other sides of the light guide are also assembled with mirrors. The light guide is attached to a heat sink to dissipate the heat generating in the phosphor. It should be noted that coating the phosphor layer to a substrate can obtain lower phosphor temperature by dissipating the heat generated in the phosphor layer to the ambient in the case that the excitation power and flux are relatively low. However, this appears to be inefficient when the excitation power and flux increase. Hence, in the high-power projection system, the phosphor layer is usually deposited onto a rotating wheel with high thermal conductivity, as shown in Fig. 17(*b*) [42]. Besides the heat conduction through the wheel, more importantly, the effective excitation area is increased and the heat density is reduced, thus leading to a lower phosphor temperature. Despite the effective heat dissipation ability of this method, the use of the rotating wheel not only increases the cost but also reduces the reliability of the whole system for long-time operation.

Alternatively, liquid cooling for the phosphor is also presented. As shown in Fig. 17(*c*), Li and Road proposed a sealed phosphor liquid cooling system consisting of a metal-sealed chamber attached with a cooling fin, a phosphor layer coated onto the top of the heat sink, cooling liquid filled with the chamber, and a compressible air chamber to compensate for the different thermal expansion of the liquid and the chamber [49]. The phosphor layer can be effectively cooled by the cycling liquid, thus obtaining very low operating phosphor temperature. However, suspending the phosphor layer in the cooling liquid may not only affect the light extraction but also reduce the reliability, which needs further designs and improvements.

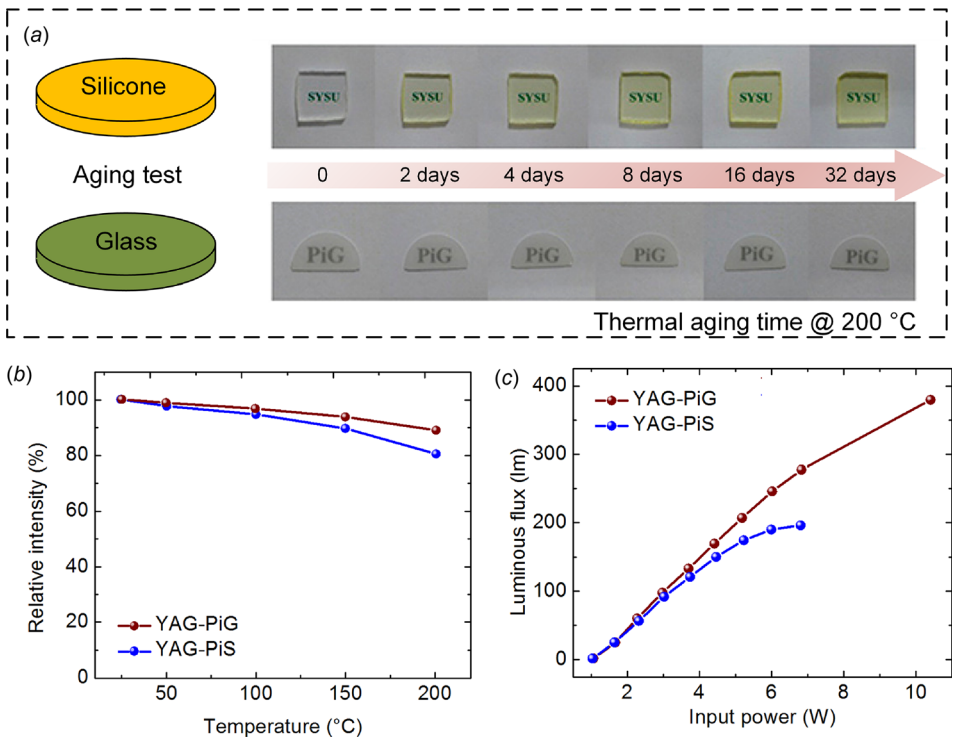

Fig. 18 (*a*) Photographs of the silicone and glass under heating temperature of 200 °C for different aging time, (*b*) the temperature dependence of the relative intensity of YAG-PiG and YAG-PiS [50], and (*c*) the luminous flux versus input power for YAG-PiG and YAG-PiS [47]

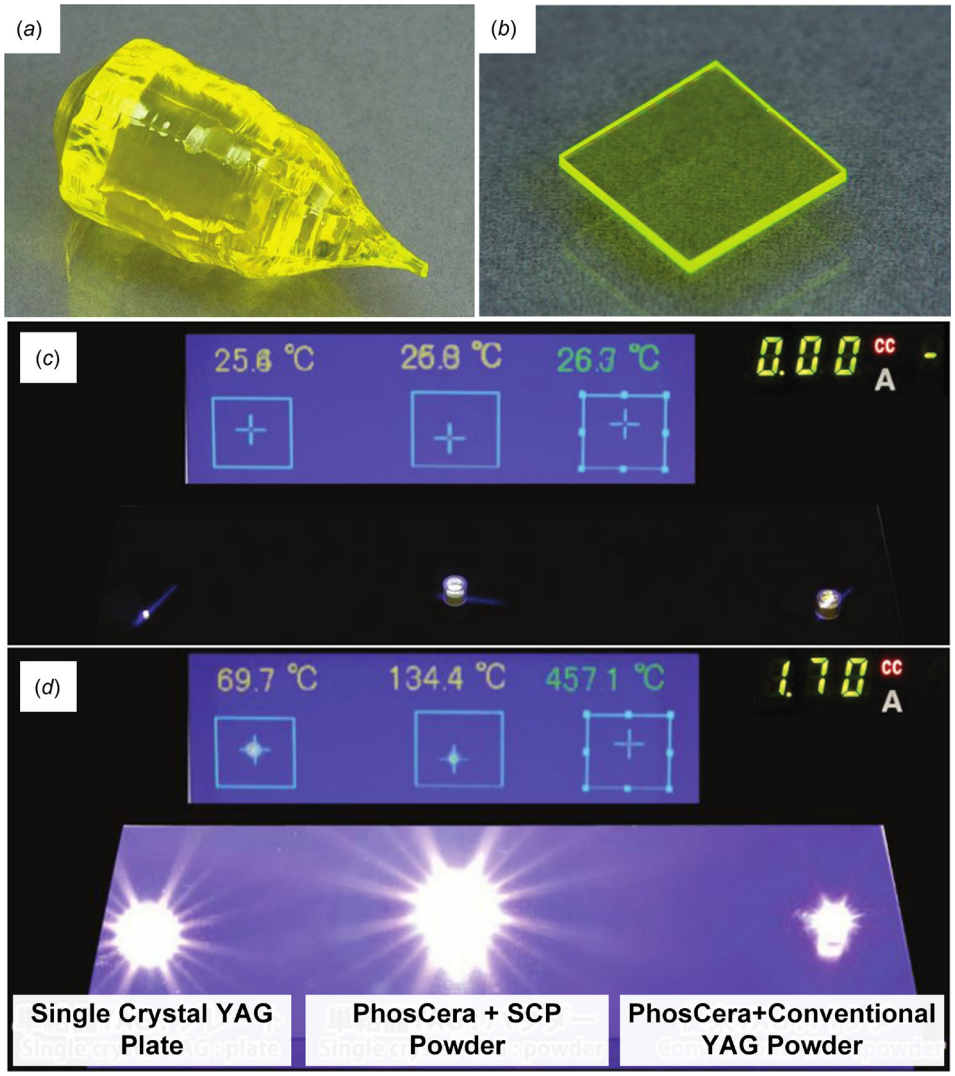

Fig. 19 (*a*) Photograph of YAG: Ce SCP grown by the Cz technique, and (*b*) fabricated SCP plate. Temperature rise of three different phosphor samples, including SCP plate, PhosCera + SCP powder, PhosCera + conventional YAG: Ce powder, under different LD input currents of (*c*) <10 mA, and (*d*) 1.7 A [100].

It should be noted there is another way of reducing phosphor temperature by redistributing heat generation distribution within the phosphor layer. Recently, Correia et al. have proposed a secondary optics design to tailor the radiation pattern from LD so that the heat generation density is skewed toward the periphery of the phosphor layer, where has the highest thermal dissipation ability [98]. Using this design, the maximum phosphor temperature was significantly reduced from 205 °C to 120 °C under exciting power of 5 W, contributing to a possible 60% higher peak luminance extracted from the laser-based light system.

4.3.2 Thermally Stable Phosphor. Typically, the phosphor layer in pc-LEDs is usually a mixture of the ceramic phosphor powder (YAG: Ce) and the organic binder (epoxy or silicone). Because of the unstable property of the organic binder at high temperature and the low thermal conductivity, this type of phosphor layer is no longer suitable for WLDs under high excitation flux. Hence, other types of phosphor materials with high thermal stability have been applied for high power WLDs.

One candidate is the phosphor-in-glass (PiG) [42,47,50,53,54,99], which is commonly synthesized by sintering the mixture of commercial phosphor powder and inorganic glass powders at an optimal temperature. By replacing the organic resins with the inorganic glass, the effective thermal conductivity of the PiG ($\sim$0.59 W m^{-1} K^{-1}) can be about three times larger than that of traditional phosphor/silicone mixture ($\sim$0.18 W m^{-1} K^{-1}) [50]. Figure 18(*a*) shows the variations of the silicone and glass heating at 200 °C at varying aging time. After 32 days, the body color of the silicone changes from colorless to browner, whereas the glass has no variation. As shown in Fig. 18(*b*), when mixed with the phosphor powders, the relative intensity under LD excitation of the glass-based phosphor (YAG-PiG) only exhibits 11.4% decrease at 200 °C, compared with 18.9% decrease for silicone-based phosphor (YAG-PiS) [50]. These all demonstrate that PiG possesses higher thermal stability than PiS. Lee et al. experimentally compared the output luminous flux of the YAG-PiG and YAG-PiS versus different input powers [47]. As shown in Fig. 18(*c*), as the input power rises, the luminous flux of both samples keep increasing. When the input power is greater than 4 W, the rising rate of YAG-PiS starts to decrease. In addition, the silicone is burnt for YAG-PiS sample at 10 W, whereas the YAG-PiG remains stable [47].

Another candidate is the single-crystal phosphor (SCP) [100,101], which is mostly grown from the melt by the Czochralski (Cz) technique. Figures 19(*a*) and 19(*b*) show the photographs of the grown single-crystal phosphor and fabricated SCP plate, respectively. The SCP exhibits very high conversion efficiency at

any temperature due to the smallest possible impurity concentration and the most regular atomic arrangement [100]. For example, the internal quantum efficiency of the YAG: Ce SCP can maintain 95% from the room temperature to 300 °C [100]. Moreover, the SCP is free-standing, which means the binders are no longer needed. In this case, the thermal instability caused by the binders can be avoided. Furthermore, the thermal conductivity of SCP ($\sim$14 W m^{-1} K^{-1}) is much higher than that of the traditional silicone-based phosphor and even PiG, enhancing the heat dissipation efficiency for the phosphor. To illustrate these advantages of SCP, the performances under LD excitation were measured. As shown in Figs. 19(*c*) and 19(*d*), three 2 W LDs were focused onto three different samples, i.e., a free-standing SCP plate, a SCP powder embedded in an inorganic binder (PhosCera), and the ceramic phosphor powder embedded in PhosCera. It can be seen that when the current reaches 1.7 A, the measured temperature of these three samples was 69.7 °C, 134.4 °C, and 457.1 °C, respectively. In this case, thermal quenching occurred for the ceramic phosphor-PhosCera sample, while the free-standing SCP sample exhibited strong thermal stability. When comparing these two candidates, the SCP obviously possesses better thermal stability than PiG. However, SCP is still facing with some major barriers including very high cost, poor reproducibility, and complex preparation procedures. In contrast, the fabrication process of PiG is simple and mature with the advantages of low cost and large scalability.

There are also other competitive candidates, such as nanostructured ceramic YAG: Ce phosphor [102], phosphor-aluminum composite [103], and YAG: Ce/Al_2O_3 composite [104–107]. They can all enhance the thermal conductivity and thermal stability of the phosphor. A comprehensive overview of the color conversion materials for laser-driven lighting has been recently presented in Ref. [108].

5 Summary and Perspectives

Laser-based white lighting has developed in the past years and made a progress especially in high-power and high-luminance solid-state lighting. In this review, we introduced the advantages of the LDs over LEDs and the applications in laser projector, automotive laser headlamp, medical endoscope, and visible light communication. Then, the packaging structure and process of WLDs were overviewed. Next, the challenges in WLD packaging were presented, including the high heat flux of LD, poor beam quality, and phosphor thermal quenching. With the objective of developing WLDs with high-luminance, color quality, and stability, researchers have been devoted to solving the packaging problems, including thermal management of LD chip to obtain low junction temperature, laser beam shaping to enhance the beam quality, and phosphor thermal management and selection of thermally stable phosphor to relieve the phosphor thermal quenching.

It should be noted that the state-of-the-art luminous efficiency of WLDs is relatively lower than that of state-of-the-art WLEDs. It is primarily due to that the power-conversion efficiency of LD is relatively low even at very higher current density. Also, the price of the commercial LD is about ten or more times than that of LEDs. Both of them limit the rapid development of WLDs. Fortunately, Wierer et al. have proposed various potential methods to improve the efficiency of LDs, including decreasing series resistance of LD, decreasing optical loss, increasing modal gain, changing crystal orientation, and improving line-shape broadening [7,8]. Figure 20 plots the power-conversion efficiency of the state-of-the-art and future LED and LD. Wierer et al. predicted that the peak efficiency of the future LD may be close to the peak efficiency of the future LED and the threshold of the future LD may also decrease. Similar to the rapid development of LED in the last decade, it is believed that the LD will also advance in the future with higher efficiency and decreasing cost, contributing to high-efficiency and high-luminance WLDs.

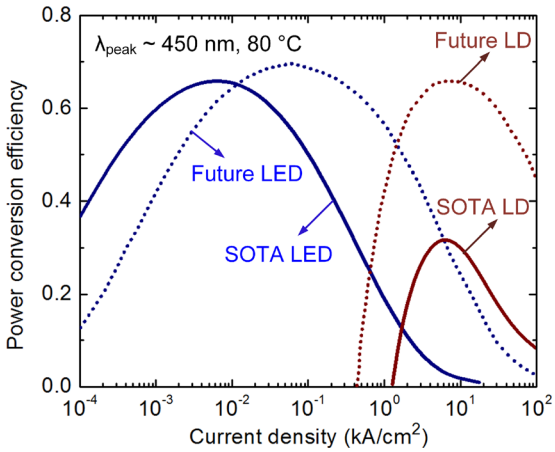

Fig. 20 The power-conversion efficiency of the state-of-the-art (SOTA) and future LED and LD [8]

In addition, high-luminance is usually achieved by collimating or focusing a small laser spot onto a phosphor layer. Most of the optical energy falls in the low angular angle, and only little energy is in the large angular angle. When the excitation light penetrates through the phosphor layer usually with a planar shape, most of the blue light will be directly transmitted without significant absorption, scattering, and conversion in the small angular angle (especially along the incident direction), whereas the blue light will be very small in the large angle. In this case, there is a large difference of the yellow to blue light ratio in the angular direction, leading to very low angular color uniformity [109]. This problem should be tackled in some applications where the uniform illumination is needed. The secondary optics design and phosphor geometry optimization may be the potential solutions.

Besides, the characteristics of a point-like source and directional emission pattern make the LDs very suitable for compact light source engines, which is exactly the developing trend for future-integrated optoelectronic devices. However, there are also some additional challenges in compact and high-luminance WLDs. Due to the limited space, the presented thermal management design with complicated and large system may no longer work efficiently. Compact and efficient cooling scheme (most possibly liquid cooling) needs to be further developed. Moreover, the size of the beam shaping optics and the secondary optics is also restricted. The increased energy density may also pose challenges in the thermal management of the phosphor layer and packaging encapsulants.

Funding Data

- National Natural Science Foundation of China (Grant Nos. 51625601, 51576078, and 51606074; Funder ID: 10.13039/501100001809).
- Creative Research Groups Funding of Hubei Province (2018CFA001; Funder ID: 10.13039/501100003999).
- Ministry of Science and Technology of the People's Republic of China (2017YFE0100600; Funder ID: 10.13039/501100002855).

References

[1] Luo, X. B., Hu, R., Liu, S., and Wang, K., 2016, "Heat and Fluid Flow in High-Power LED Packaging and Applications," Prog. Energy Combus. Sci., **56**, pp. 1–32.

[2] Xie, B., Hu, R., and Luo, X. B., 2016, "Quantum Dots-Converted Light-Emitting Diodes Packaging for Lighting and Display: Status and Perspectives," ASME J. Electron. Packag., **138**(2), p. 020803.

[3] Ma, Y. P., Hu, R., Yu, X. J., Shu, W. C., and Luo, X. B., 2017, "A Modified Bidirectional Thermal Resistance Model for Junction and Phosphor

Temperature Estimation in Phosphor-Converted Light-Emitting Diodes," Int. J. Heat Mass Transfer, **106**, pp. 1–6.
[4] Schubert, E. F., Kim, J. K., Luo, H., and Xi, J. Q., 2006, "Solid State Lighting–A Benevolent Technology," Rep. Prog. Phys., **69**(12), pp. 3069–3099.
[5] Maur, M. A. D., Pecchia, A., Penazzi, G., Rodrigues, W., and Carlo, A. D., 2016, "Efficiency Drop in Green InGaN/GaN Light Emitting Diodes: The Role of Random Alloy Fluctuations," Phys. Rev. Lett., **116**(2), p. 027401.
[6] Cantore, M., Pfaff, N., Farrell, R. M., Speck, J. S., Nakamura, S., and DenBaars, S. P., 2016, "High Luminous Flux From Single Crystal Phosphor-Converted Laser-Based White Lighting System," Opt. Exp., **24**(2), p. A215.
[7] Wierer, J. J., Tsao, J. Y., and Sizov, D. S., 2013, "Comparison Between Blue Lasers and Light-Emitting Diodes for Future Solid-State Lighting," Laser Photonics Rev., **7**(6), pp. 963–993.
[8] Wierer, J. J., and Tsao, J. Y., 2015, "Advantages of III-Nitride Laser Diodes in Solid-State Lighting," Phys. Status Solidi A, **212**(5), pp. 980–985.
[9] Nakamura, S., 2015, "Background Story of the Invention of Efficient Blue InGaN Light Emitting Diodes," Int. J. Mod. Phys. B, **29**(32), p. 1530016.
[10] Basu, C., Wollweber, M. M., and Roth, B., 2013, "Lighting With Laser Diodes," Adv. Opt. Technol., **2**(4), pp. 313–321.
[11] Ma, Y. P., Lan, W., Xie, B., Hu, R., and Luo, X. B., 2018, "An Optical-Thermal Model for Laser-Excited Remote Phosphor With Thermal Quenching," Int. J. Heat Mass Transfer, **116**, pp. 694–702.
[12] Neumann, A., Wierer, J. J., Davis, W., Ohno, Y., Brueck, S. R. J., and Tsao, J. Y., 2011, "Four-Color Laser White Illuminant Demonstrating High Color-Rendering Quality," Opt. Express, **19**(S4), p. A982.
[13] Hung, P. C., and Tsao, J. Y., 2013, "Maximum White Luminous Efficacy of Radiation Versus Color Rendering Index and Color Temperature: Exact Results and a Useful Analytic Expression," J. Disp. Technol., **9**(6), pp. 405–412.
[14] Chellappan, K. V., Erden, E., and Urey, H., 2010, "Laser-Based Displays: A Review," Appl. Opt., **49**(25), pp. F79–F98.
[15] Nippon Electronic Company, 2019, "What is Laser," Nippon Electronic Company, Tokyo, Japan, accessed Aug. 5, 2019, https://www.necdisplay.com/laser-projectors/laser.html
[16] Wierer, J. J., Tsao, J. Y., and Sizov, D. S., 2014, "The Potential of III-Nitride Laser Diodes for Solid-State Lighting," Phys. Status Solidi C, **11**(3–4), pp. 674–677.
[17] Ulrich, L, 2013, "BMW Laser Headlights Slice Through the Dark," BMW, Munich, Germany, accessed Aug. 5, 2019, https://spectrum.ieee.org/transportation/advanced-cars/bmw-laser-headlights-slice-through-the-dark?tdsourcetag=s_pcqq_aiomsg
[18] Wanka, J., 2017, "Photonics in Germany," Munich, Germany, Germany, accessed Aug. 5, 2019, https://agustos.com/wp-content/uploads/2018/07/BMW-Article-Photonics-in-Germany-2017.pdf
[19] Max, 2017, "Laser headlight in automotive lighting," Audi, Ingolstadt, Germany, accessed Aug. 5, 2019, http://www.serafim-tech.com/blog/laser-headlight-in-automotive-lighting.html?tdsourcetag=s_pcqq_aiomsg
[20] Volpe, J., 2004, "Mercedes-Benz GLA concept puts laser projectors in headlights, redefines SUV," Girard, PA, accessed Aug. 5, 2019, http://www.engadget.com/2013/04/18/mercedes-benz-gla-concept-puts-laser-projectors-in-headlights/
[21] Nadeau, V. J., Elson, D. S., Neil, M. A. A., and Hanna, G. B., 2008, "Laser-Pumped Endoscopic Illumination Source," 30th Annual International Conference of the IEEE Engineering in Medicine and Biology Society, Vancouver, BC, Canada, Aug. 20–25, pp. 2059–2062.
[22] Chi, Y. C., Hsieh, D. H., Lin, C. Y., Chen, H. Y., Huang, C. Y., He, J. H., Ooi, B., DenBaars, S. P., Nakamura, S., Kuo, H. C., and Lin, G. R., 2015, "Phosphorous Diffuser Diverged Blue Laser Diode for Indoor Lighting and Communication," Sci. Rep., **5**, p. 18690.
[23] Retamal, J. R. D., Oubei, H. M., Janjua, B., Chi, Y., Wang, H., Tsai, C., Ng, T. K., Hsieh, D., Kuo, H. C., Alouini, M., He, J., Lin, G., and Ooi, B. S., 2015, "4-Gbit/s Visible Light Communication Link Based on 16-QAM OFDM Transmission Over Remote Phosphor-Film Converted White Light by Using Blue Laser Diode," Opt. Express, **23**(26), pp. 33656–33666.
[24] Chi, Y. C., Huang, Y. F., Wu, T. C., Tsai, C. T., Chen, L. Y., Kuo, H. C., and Lin, G. R., 2017, "Violet Laser Diode Enables Lighting Communication," Sci. Rep., **7**, p. 10469.
[25] Aquino, F., Jadwisienczak, W. M., and Rahman, F., 2017, "Effect of Laser Speckle on Light From Laser Diode-Pumped Phosphor-Converted Light Sources," Appl. Opt., **56**(2), pp. 278–283.
[26] Zhao, Z., Mhibik, O., Leang, T., Forget, S., and Chénais, S., 2014, "Thermal Effects in Thin-Film Organic Solid-State Lasers," Opt. Express, **22**(24), pp. 30092–30107.
[27] Lenef, A., Kelso, J., Zheng, Y., and Tchoul, M., 2013, "Radiance Limits of Ceramic Phosphors Under High Excitation Fluxes," *Current Developments in Lens Design and Optical Engineering XIV*, International Society for Optics and Photonics, San Diego, CA, pp. 884107–884120.
[28] Liu, X., Zhao, W., Xiong, L., and Liu, H., 2015, *Packaging of High Power Semiconductor Lasers*, Springer, New York.
[29] Wu, T. C., Chi, Y. C., Wang, H. Y., Tsai, C. T., Huang, Y. F., and Lin, G. R., 2017, "Tricolor R/G/B Laser Diode Based Eye-Safe White Lighting Communication Beyond 8 Gbit/s," Sci. Rep., **7**(1), p. 11.
[30] Reitterer, J., Fidler, F., Hambeck, C., Julien-Wallsee, F. S., Najda, S., Perlin, P., Stanczyk, S., Czernecki, R., McDougall, S. D., Meredith, W., Vickers, G., Landles, K., and Schmid, U., 2015, "Integrated RGB Laser Light Module for Autostereoscopic Outdoor Displays," SPIE Proc., **9346**, p. 934619.
[31] Yang, J., Liu, Z., Xue, B., Liao, Z., Feng, L., Zhang, N., Wang, J. X., and Li, J. M., 2018, "Highly Uniform White Light-Based Visible Light Communication Using Red, Green, and Blue Laser Diodes," IEEE Photonics J., **10**(2), pp. 1–8.
[32] Huang, Y. F., Chi, Y. C., Chen, M. K., Tsai, D. P., Huang, D. W., and Lin, G. R., 2018, "Red/Green/Blue LD Mixed White-Light Communication at 6500K With Divergent Diffuser Optimization," Opt. Express, **26**(18), pp. 23397–23410.
[33] Xu, Y., Chen, L. H., Li, Y. Z., Song, G. F., Wang, Y. P., Zhuang, W. D., and Long, Z., 2008, "Phosphor-Conversion White Light Using InGaN Ultraviolet Laser Diode," Appl. Phys. Lett., **92**(2), p. 021129.
[34] Hu, F., and Li, Y., 2013, "Laser and Phosphor Hybrid Source for Projection Display," SPIE Paper No. 85991K.
[35] Denault, K. A., Cantore, M., Nakamura, S., Denbaars, S. P., and Seshadri, R., 2013, "Efficient and Stable Laser-Driven White Lighting," AIP Adv., **3**(7), p. 072107.
[36] Abu-Ageel, N., Aslam, D., and Member, S., 2014, "Laser-Driven Visible Solid-State Light Source for Etendue-Limited Applications," J. Disp. Technol., **10**(8), pp. 700–703.
[37] George, A. F., Al-Waisawy, S., Wright, J. T., Jadwisienczak, W. M., and Rahman, F., 2016, "Laser-Driven Phosphor-Converted White Light Source for Solid-State Illumination," Appl. Opt., **55**(8), pp. 1899–1905.
[38] Al-Waisawy, S., Jadwisienczak, W. M., Wright, J. T., Pendrill, D., and Rahman, F., 2016, "Laser Excitation of Red, Green, Blue and Trichromatic White Rare-Earth Phosphors for Solid-State Lighting Applications," J. Lumin., **169**, pp. 196–203.
[39] Lee, C. M., Shen, C., Cozzan, C., Farrell, R. M., Speck, J. S., Nakamura, S., Ooi, B. S., and DenBaars, S. P., 2017, "Gigabit-Per-Second White Light-Based Visible Light Communication Using Near-Ultraviolet Laser Diode and Red-, Green-, and Blue-Emitting Phosphors," Opt. Express, **25**(15), pp. 17480–17487.
[40] Ryu, H. Y., and Kim, D. H., 2010, "High-Brightness Phosphor-Conversion White Light Source Using InGaN Blue Laser Diode," J. Opt. Soc. Korea, **14**(4), pp. 415–419.
[41] Xu, Y., Hu, H., Chen, L., Song, G., and Zhuang, W., 2010, "Analysis on the High Luminous Flux White Light From GaN-Based Laser Diode," Appl. Phys. B: Lasers Opt., **98**(1), pp. 83–86.
[42] Chang, J. K., Cheng, W. C., Chang, Y. P., Kuo, Y. Y., Tsai, C. C., Huang, Y. C., Chen, L. Y., and Cheng, W. H., 2015, "Next-Generation Glass-Base Phosphor-Converted Laser Light Engine," SPIE Proc., **9571**, p. 957103.
[43] Masui, S., Yamamoto, T., and Nagahama, S., 2015, "A White Light Source Excited by Laser Diodes," Electron. Commun. Jpn., **98**(5), pp. 23–27.
[44] Farooq, T., and Qian, K., 2015, "High Luminance Low Etendue White Light Source Using Blue Laser Over Static Phosphor," SPIE Paper No. 96710C.
[45] Lee, D. H., Joo, J., and Lee, S., 2015, "Modeling of Reflection-Type Laser-Driven White Lighting Considering Phosphor Particles and Surface Topography," Opt. Express, **23**(15), pp. 18872–18887.
[46] Salimian, A., Fern, G. R., Upadhyaya, H., and Silver, J., 2016, "Laser Diode Induced Lighting Modules," ECS J. Solid State Sci. Technol., **5**(3), pp. R26–R33.
[47] Lee, T.-X., Chou, C.-C., and Chang, S.-C., 2016, "Novel Remote Phosphor Design for Laser-Based White Lighting Application," SPIE Paper No. 99540O.
[48] Salimian, A., Silver, J., Fern, G. R., Evans, M., and Haghpanahan, R., 2016, "Evaluation of Thermally Stable Phosphor Screens for Application in Laser Diode Excited High Brightness White Light Modules," ECS J. Solid State Sci. Technol., **5**(1), pp. R3001–R3006.
[49] Li, K., and Road, T. O., 2017, "High-Power Laser Phosphor Light Source With Liquid Cooling for Digital Cinema Applications," SPIE Proc., **9005**, p. 900507.
[50] Zhang, X., Yu, J., Wang, J., Lei, B., Liu, Y., Cho, Y., Xie, R., Zhang, H., Li, Y., Tian, Z., Li, Y., and Su, Q., 2017, "All-Inorganic Light Convertor Based on Phosphor-in-Glass Engineering for Next-Generation Modular High-Brightness White LEDs/LDs," ACS Photonics, **4**(4), pp. 986–995.
[51] Yang, J., Liu, Z., Xue, B., Wang, J., and Li, J., 2017, "Research on Phosphor-Conversion Laser-Based White Light Used as Optical Source of VLC and Illumination," Opt. Quantum Electron., **49**(4), p. 173.
[52] Yang, Y., Zhuang, S. L., and Kai, B. C., 2017, "High Brightness Laser-Driven White Emitter for Etendue-Limited Applications," Appl. Opt., **56**(30), pp. 8321–8325.
[53] Zheng, P., Li, S. X., Wang, L., Zhou, T. L., You, S. H., Takeda, T., Hirosaki, N., and Xie, R. J., 2018, "Unique Color Converter Architecture Enabling Phosphor-in-Glass (PiG) Films Suitable for High-Power and High-Luminance Laser-Driven White Lighting," ACS Appl. Mater. Inter., **10**(17), pp. 14930–14940.
[54] Peng, Y., Mou, Y., Wang, H., Zhuo, Y., Li, H., Chen, M., and Luo, X., 2018, "Stable and Efficient All-Inorganic Color Converter Based on Phosphor in Tellurite Glass for Next-Generation Laser-Excited White Lighting," J. Eur. Ceram. Soc., **38**(16), pp. 5525–5532.
[55] Peng, Y., Mou, Y., Sun, Q. L., Cheng, H., Chen, M. X., and Luo, X. B., 2019, "Facile Fabrication of Heat-Conducting Phosphor-in-Glass With Dual-Sapphire Plates for Laser-Driven White Lighting," J. Alloys Compd., **790**, pp. 744–749.
[56] Lee, D. H., Kim, S., Kim, H., and Lee, S. K., 2019, "Highly Efficient and Highly Conductive Phosphor-in-Glass Materials for Use in LD-Driven White-Light Lamp," Int. J. Precis. Eng. Manuf. Green Technol., **6**, pp. 293–303.

[57] Zhang, X. J., Si, S. C., Yu, J. B., Wang, Z. J., Zhang, R. H., Lei, B. F., Liu, Y. L., Zhuang, J. L., Hu, C. F., Cho, Y. J., Xie, R. J., Zhang, H. W., Tian, Z. F., and Wang, J., 2019, "Improving the Luminous Efficacy and Resistance to Blue Laser Irradiation of Phosphor-in-Glass Based Solid State Laser Lighting Through Employing Dual-Functional Sapphire Plate," J. Mater. Chem. C, **7**(2), pp. 354–361.

[58] Ma, Y. P., Wang, M., and Luo, X. B., 2018, "A Comparative Study of Reflective and Transmissive Phosphor-Converted Laser-Based White Lighting," 17th IEEE Intersociety Conference on Thermal and Thermomechanical Phenomena in Electronic Systems (ITherm), San Diego, May 29–June 1, pp. 773–777.

[59] Lenef, A., Kelso, J., Tchoul, M., Mehl, O., Sorg, J., and Zheng, Y., 2014, "Laser-Activated Remote Phosphor Conversion With Ceramic Phosphors," SPIE Paper No. 91900C.

[60] Rao, R. P., 1996, "Growth and Characterization of Y_2O_3: Eu^{3+} Phosphor Films by Sol-Gel Process," Solid State Commun., **99**(6), pp. 439–443.

[61] Luo, X. B., Mao, Z. M., Yang, J., and Liu, S., 2012, "Engineering Method for Predicting Junction Temperatures of High-Power Light-Emitting Diodes," IET Optoelectron., **6**(5), pp. 230–236.

[62] Ma, Y. P., Wang, M., Sun, J., Hu, R., and Luo, X. B., 2018, "Phosphor Modeling Based on Fluorescent Radiative Transfer Equation," Opt. Express, **26**(13), pp. 16442–16455.

[63] Bacchin, G., Fily, A., Qiu, B., Fraser, D., Robertson, S., Loyo-Maldonado, V., McDougall, S. D., and Schmidt, B., 2010, "High Temperature and High Peak Power 808 nm QCW Bars and Stacks," SPIE Proc., **7583**, p. 75830P.

[64] Fan, L., Cao, C. S., Thaler, G., Nonnemacher, D., Lapinski, F., Ai, I., Caliva, B., Das, S., Walker, R., Zeng, L. F., McElhinney, M., and Thiagarajan, P., 2011, "Reliable High-Power Long-Pulse 8XX-nm Diode Laser Bars and Arrays Operating at High Temperature," SPIE Proc., **7918**, p. 791805.

[65] Serkan, M., and Kirkici, H., 2009, "Reshaping of a Divergent Elliptical Gaussian Laser Beam Into a Circular, Collimated, and Uniform Beam With Aspherical Lens Design," IEEE Sens. J., **9**(1), pp. 36–44.

[66] Diehl, R. D., and Diehl, R. L., 2000, *High-Power Diode Lasers: Fundamentals, Technology, Applications*, Springer Science and Business Media, New York.

[67] Duna, K., and Lu, B., 2004, "Propagation Properties of Vector Elliptical Gaussian Beams Beyond the Paraxial Approximation," Opt. Laser Technol., **36**(6), pp. 489–496.

[68] Ueda, J., Dorenbos, P., Bos, A. J. J., Meijerink, A., and Tanabe, S., 2015, "Insight Into the Thermal Quenching Mechanism for $Y_3Al_5O_12$:Ce^{3+} Through Thermoluminescence Excitation Spectroscopy," J. Phys. Chem. C, **119**(44), pp. 25003–25008.

[69] Luo, X. B., Fu, X., Chen, F., and Zheng, H., 2013, "Phosphor Self-Heating in Phosphor Converted Light Emitting Diode Packaging," Int. J Heat Mass Transf., **58**(1–2), pp. 276–281.

[70] Bachmann, V., Ronda, C., and Meijerink, A., 2009, "Temperature Quenching of Yellow Ce^{3+} Luminescence in YAG:Ce," Chem. Mater., **21**(10), pp. 2077–2084.

[71] Hu, R., and Luo, X. B., 2012, "A Model for Calculating the Bidirectional Scattering Properties of Phosphor Layer in White Light-Emitting Diodes," J. Lightwave Technol., **30**(21), pp. 3376–3380.

[72] Luo, X. B., and Hu, R., 2014, "Calculation of the Phosphor Heat Generation in Phosphor-Converted Light-Emitting Diodes," Int. J. Heat Mass Transfer, **75**, pp. 213–217.

[73] Ma, Y. P., Cheng, Y. H., Shu, W. C., Liu, F. L., Hu, R., and Luo, X. B., 2017, "A Comparative Study of Phosphor Scattering Model for Phosphor-Converted Light-Emitting Diodes," 18th International Conference on Electronic Packaging Technology (ICEPT), Harbin, China, Aug. 16–19, pp. 389–393.

[74] Ma, Y. P., and Luo, X. B., 2019, "Two-Dimensional Axisymmetric Opto-Thermal Phosphor Modeling Based on Fluorescent Radiative Transfer Equation," J. Lumin., **214**, p. 116589.

[75] Li, X. N., Peng, C. H., Zhang, Y. X., Wang, J. W., Xiong, L. L., Zhang, P., and Liu, X. S., 2010, "A New Continuous Wave 2500 W Semiconductor Laser Vertical Stack," 11th International Conference on Electronic Packaging Technology and High Density Packaging, Xi'an, China, Aug. 16–19, pp. 1350–1354.

[76] Zweben, C., 2005, "New Low-CTE Ultrahigh-Thermal-Conductivity Materials for Lidar Laser Diode Packaging," SPIE Proc., **5887**, p. 58870D.

[77] Shang, B. F., Ma, Y. P., Hu, R., Yuan, C., Hu, J. Y., and Luo, X. B., 2017, "Passive Thermal Management System for Downhole Electronics in Harsh Thermal Environments," Appl. Therm. Eng., **118**, pp. 593–599.

[78] Lee, Y. H., Park, S., Byun, C., and Lee, S. K., 2018, "Liquid Cooling of Laser-Driven Head Light Employing Heat Spreader Manufactured by 3D Metal Printing," Int. J. Precis. Eng. Manuf. Green Technol., **5**(2), pp. 295–301.

[79] Zhao, D., and Tan, G., 2014, "A Review of Thermoelectric Cooling: Materials, Modeling and Applications," Appl. Therm. Eng., **66**(1–2), pp. 15–24.

[80] Datta, M., and Choi, H. W., 2015, "Microheat Exchanger for Cooling High Power Laser Diodes," Appl. Therm. Eng., **90**, pp. 266–273.

[81] Kozłowska, A., Łapka, P., Seredyński, M., Teodorczyk, M., and Dąbrowska-Tumańska, E., 2015, "Experimental Study and Numerical Modeling of Micro-Channel Cooler With Micro-Pipes for High-Power Diode Laser Arrays," Appl. Therm. Eng., **91**, pp. 279–287.

[82] Baraty, S., Bahrami, A., and Reza, M., 2017, "Design of Novel Geometries for Microchannel Heat Sinks Used for Cooling Diode Lasers," Int. J. Heat Mass Transf., **112**, pp. 689–698.

[83] Hoffnagle, J. A., and Jefferson, C. M., 2000, "Design and Performance of a Refractive Optical System That Converts a Gaussian to a Flattop Beam," Appl. Opt., **39**(30), pp. 5488–5499.

[84] Oliker, V., 2007, "Optical Design of Freeform Two-Mirror Beam-Shaping Systems," J. Opt. Soc. Am. A, **24**(12), pp. 3741–3752.

[85] Palima, D., and Glückstad, J., 2008, "Gaussian to Uniform Intensity Shaper Based on Generalized Phase Contrast," Opt. Express, **16**(3), pp. 1507–1516.

[86] Dresel, T., Beyerlein, M., and Schwider, J., 1996, "Design and Fabrication of Computer-Generated Beam-Shaping Holograms," Appl. Opt., **35**(23), pp. 4615–4621.

[87] Hoque, M. U., Hasan, M. N., and Lee, Y. C., 2017, "Design and Fabrication of a Biconvex Aspherical Microlens for Maximizing Fiber Coupling Efficiency With an Ultraviolet Laser Diode," Sens. Actuators A-Phys., **254**, pp. 36–42.

[88] Hasan, M. N., Haque, M. U., Trisno, J., and Lee, Y. C., 2015, "Direct-Writing Lithography Using Laser Diode Beam Focused With Single Elliptical Microlens," J. Micro-Nanolithogr., MEM, MOEMS, **14**(4), p. 43505.

[89] Hasan, M. N., Haque, M. U., and Lee, Y. C., 2016, "Deastigmatism, Circularization, and Focusing of a Laser Diode Beam Using a Single Biconvex Microlens," Opt. Eng., **55**(9), p. 095107.

[90] Romero, L. A., and Dickey, F. M., 1996, "Lossless Laser Beam Shaping," J. Opt. Soc. Am. A, **13**(4), pp. 751–760.

[91] Li, M., Meuret, Y., Duerr, F., Vervaeke, M., and Thienpont, H., 2014, "Comprehensive Numerical Design Approach for Refractive Laser Beam Shapers to Generate Annular Irradiance Profiles," Opt. Eng., **53**(8), p. 085103.

[92] Serkan, M., and Kirkici, H., 2008, "Optical Beam-Shaping Design Based on Aspherical Lenses for Circularization, Collimation, and Expansion of Elliptical Laser Beams," Appl. Opt., **47**(2), pp. 230–241.

[93] Zhou, X. Q., Ann, B. N., and Seong, K. S., 2000, "Single Aspherical Lens for Deastigmatism, Collimation, and Circularization of a Laser Beam," Appl. Opt., **39**(7), pp. 1148–1151.

[94] Zhang, S., Neil, G., and Shinn, M., 2003, "Single-Element Laser Beam Shaper for Uniform Flat-Top Profiles," Opt. Express, **11**(16), pp. 1942–1948.

[95] Yeh, S. M., Huang, S. Y., and Cheng, W. H., 2005, "A New Scheme of Conical-Wedge-Shaped Fiber End Face for Coupling Between High-Power Laser Diodes and Single-Mode Fibers," J. Lightwave Technol., **23**(4), pp. 1781–1786.

[96] Kawano, K., 1986, "Coupling Characteristics of Lens Systems for Laser Diode Modules Using Single-Mode Fiber," Appl. Opt., **25**(15), pp. 2600–2605.

[97] Palais, J. C., 1980, "Fiber Coupling Using Graded-Index Rod Lenses," Appl. Opt., **19**(12), pp. 2011–2018.

[98] Correia, A., Hanselaer, P., and Meuret, Y., 2019, "Improving the Opto-Thermal Performance of Transmissive Laser-Based White Light Sources Through Beam Shaping," Opt. Express, **27**(8), pp. A235–A244.

[99] Chang, Y. P., Chang, J. K., Cheng, W. C., Kuo, Y. Y., Liu, C. N., Chen, L. Y., and Cheng, W. H., 2017, "New Scheme of a Highly-Reliable Glass-Based Color Wheel for Next-Generation Laser Light Engine," Opt. Mater. Express, **7**(3), pp. 1029–1034.

[100] Víllora, E. G., Arjoca, S., Inomata, D., and Shimamura, K., 2016, "Single-Crystal Phosphors for High-Brightness White LEDs/LDs," SPIE Proc., **9768**, p. 976805.

[101] Kang, T. W., Park, K. W., Ryu, J. H., Lim, S. G., Yu, Y. M., and Kim, J. S., 2017, "Strong Thermal Stability of $Lu_3Al_5O_{12}$:Ce^{3+} Single Crystal Phosphor for Laser Lighting," J. Lumin., **191**, pp. 3–7.

[102] Song, Y. H., Ji, E. K., Jeong, B. W., Jung, M. K., Kim, E. Y., and Yoon, D. H., 2016, "High Power Laser-Driven Ceramic Phosphor Plate for Outstanding Efficient White Light Conversion in Application of Automotive Lighting," Sci. Rep., **6**, p. 31206.

[103] Park, J., Kim, J., and Kwon, H., 2017, "Phosphor-Aluminum Composite for Energy Recycling With High-Power White Lighting," Adv. Opt. Mater., **5**(19), p. 1700347.

[104] Li, S., Zhu, Q., Tang, D., Liu, X., Ouyang, G., Cao, L., Hirosaki, N., Nishimura, T., Huang, Z., and Xie, R., 2016, "Al_2O_3–YAG:Ce Composite Phosphor Ceramic: A Thermally Robust and Efficient Color Converter for Solid State Laser Lighting," J. Mater. Chem. C, **4**(37), pp. 8648–8654.

[105] Song, Y. H., Ji, E. K., Jeong, B. W., Jung, M. K., Kim, E. Y., Lee, C. W., and Yoon, D. H., 2017, "Design of Laser-Driven High-Efficiency Al_2O_3/YAG:Ce^{3+} Ceramic Converter for Automotive Lighting: Fabrication, Luminous Emittance, and Tunable Color Space," Dyes Pigm., **139**, pp. 688–692.

[106] Cozzan, C., Lheureux, G., O'Dea, N., Levin, E. E., Graser, J., Sparks, T. D., Nakamura, S., DenBaars, S. P., Weisbuch, C., and Seshadri, R., 2018, "Stable, Heat-Conducting Phosphor Composites for High-Power Laser Lighting," ACS Appl. Mater. Inter., **10**(6), pp. 5673–5681.

[107] Xu, M., Chang, J., Wang, J., Wu, C., and Hu, F., 2019, "Al_2O_3-YAG:Ce Composite Ceramics for High-Brightness Lighting," Opt. Express, **27**(2), pp. 872–885.

[108] Li, S. X., Wang, L., Hirosaki, N., and Xie, R. J., 2018, "Color Conversion Materials for High-Brightness Laser-Driven Solid-State Lighting," Laser Photonics Rev., **12**(12), p. 1800173.

[109] Ma, Y. P., and Luo, X. B., 2019, "Small-Divergent-Angle Uniform Illumination With Enhanced Luminance of Transmissive Phosphor-Converted White Laser Diode by Secondary Optics Design," Opt. Laser Eng., **122**, pp. 14–22.